

Characteristics of three-phase controllable reactor under orthogonal field¹

ZHENGRONG JIANG², ZHENKUN SUN², YUNBO LIU²

Abstract. To solve the problem of additional losses, instability and harmonic currents in fixed reactors, a three-phase controllable reactor is studied by means of physical and electrical methods. The three-phase controllable reactor is based on the quadrature magnetizing energy to provide three-phase bias inductance. When the DC bias current changes, the input impedance of the three-phase reactor can be variable reactance to maintain three-phase balance. In addition, the relationship between three-phase harmonic characteristics and control is also interrelated. The magnetic mechanism of three-phase reactor under orthogonal magnetic field is introduced. A domain motion model is established. The permeability of tensor is calculated and its harmonic characteristics are analyzed. A prototype of three-phase controllable reactor is proposed, and its control characteristics are discussed. The calculated results are in good agreement with the experimental results.

Key words. B-H loop cluster, orthogonal field, tensor permeability, controllable reactor.

1. Introduction

Controllable reactor is an important equipment in power line and distribution system. Traditionally, discrete fixed shunt reactors are installed on power transmission lines and switched in or out according to the system loading. But a fixed reactor has some drawbacks, such as extra losses, less capacity of voltage stability and harmonic current generation [1]. If the fixed reactor is substituted with a controllable one, the compensation reactive power can be adjusted according to the needs of the load of the transmission and thus leads to the following advantages: lower transmission losses, higher transmission capacity of active power and less harmonics injection to the system.

¹This work was sponsored by National Natural Science Foundation of China (51377006) and Beijing Natural Science Foundation (3132008).

²School of Electrical and Control Engineering, North China University of Technology, Beijing, 100144, China

There are two types of controllable reactors as an alternative to the fixed reactor: Magnetically Controlled Reactor (MCR) and Thyristor Controlled Reactor (TCR). The main difference between MCR and TCR is that MCR changes the reactance by adjusting the permeability of the iron core of the reactor, while TCR usually depends on the current through the reactor. The latter employs some power electronics to control current but results in extra harmonic current [2].

From the viewpoint of application, TCR-based SVC are suitable for some high voltage situations, such as 220 kV and below. There are some difficulties for their applications in EHV/UHV line due to the cost and insulation problems. In these cases, the MCR-based SVC has significance advantages in respect of the cost and insulation.

MCRs can be sorted into two types according to the relative direction of the DC flux and AC flux which role as DC bias control flux and main working flux, respectively. One is called Magnetic Controlled Reactor in which DC flux direction is parallel with AC flux, and the other is called orthogonal flux reactor in which DC flux direction is orthogonal with AC flux. The latter is named as MCR+ for the difference with the former one, where the “+” signal is for the orthogonal magnetization.

2. State of the art

A controllable saturation reactor generally consists of two windings on an iron core. One of the windings, which is excited by DC current source, is called control winding; another winding is the main AC working winding, which is excited by AC voltage. Changing the DC current can adjust the saturation of the iron and the reactance of the main winding [3].

Because the reactor is based on the controlled saturation in part of the magnetic circuit, the permeability and saturation are two of the critical magnetic properties [4]. A constant permeability is nearly a flat magnetization curve across the origin of the $\mathbf{B} - \mathbf{H}$ plane, and saturation magnetization at a high field can be described by a horizontal line in the $\mathbf{B} - \mathbf{H}$ plot. When the DC bias current is changing, the magnetization curve will change gradually from the constant permeability regime to the saturation one. Therefore, the core operating point must be considered in order to accurately change the permeability of the core and the reactance of the reactor [5].

The working principle of three-phase MCR and saturable reactor is the use of magnetic saturation principle, the effect of excitation DC current to change magnetic work point and magnetic properties, magnetic saturation control degree, thus changing the reactance value of AC winding to smooth the self adjusting reactor capacity.

Although MCR is developed from the traditional controllable saturable reactor, it has its own characteristics, mainly in the following aspects:

Without external DC excitation, the traditional controllable saturable reactor needs an external large capacity DC excited power supply, while the MCR itself is DC excited by the commutation of the lotus root and controlled by silicon rectifier.

The main and control winding mutual traditional saturated controllable AC wind-

ing and DC control winding of the reactor from around the core, and the working winding and control winding MCR interoperability, not only simplified the structure, save material, and reduce the loss.

The volt ampere characteristics of saturable reactor special structure of the magnetic valve with traditional nonlinear, and MCR because of its small section core, namely the magnetic valve structure, when working, the volt ampere characteristics of the magnetic valve section is only nonlinear saturation, while the remaining section is in unsaturated linear state. This reduces the harmonic content and loss, and improves the response speed.

Single phase double column MCR, because the two AC winding in parallel, winding direction, through the core of the magnetic flux direction is the same, so must add side choke, can make AC flux loop. But the three-phase six column MCR, because its three-phase voltage is symmetrical, in the magnetic circuit the three-phase alternating current magnetic flux size is equal, the phase difference is 120 degrees. Thus, in the upper and lower iron chokes, the magnetic flux vector and zero, no excess harmonic, and no need to add a side choke to form a loop, the three-phase winding adopts triangle connection mode, and can also filter the third harmonic. Compared with three single-phase combination MCR, the three-phase MCR reduces the harmonic content, saves the material, reduces the occupation area, and improves the economic benefit to a great extent.

2.1. Methodology

The theory of controllable saturation reactor is shown as following Fig. 1.

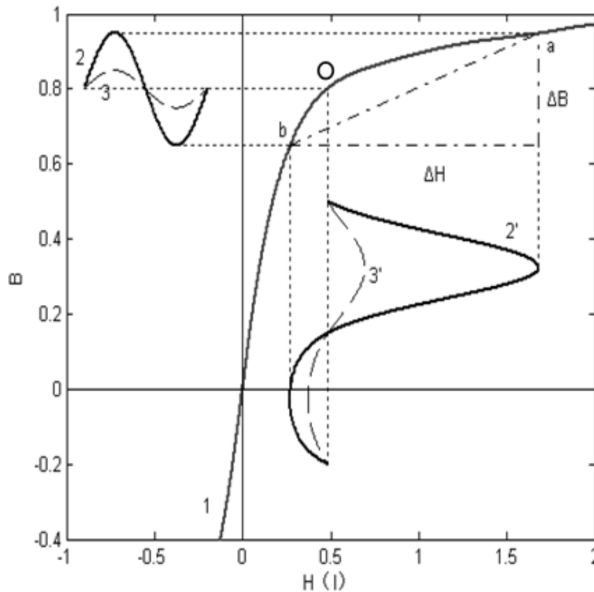


Fig. 1. Theory of saturation controllable reactor

When the operating point close to the non-linear region of the $B - H$ curve, a harmonic current is created inescapably. For example, the point is moving from b to a , the output current waveform is changed from $3'$ to $2'$. It is obvious that the non-linearity of the magnetization curve leads to a substantial harmonic distortion.

When the operating points are retained in the linear region of the $B - H$ "cluster", the output current waveform can be expected to maintain sinusoidal in a wide control region [6], as shown in Fig. 2.

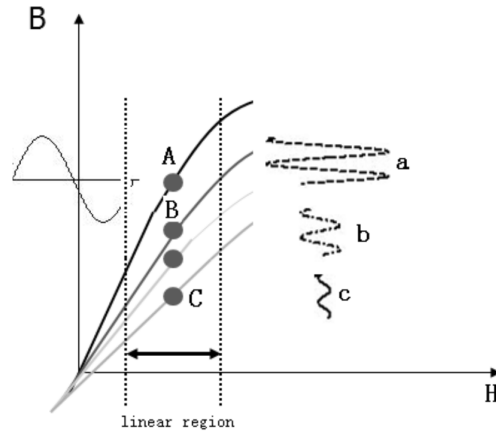


Fig. 2. Operating points in linear region results in sinusoidal waveform

When the DC bias current is changing, the magnetization curve should be decided in the cluster of $B - H$ plane, which maintains in the linear area, so the changing accurately reactance of the reactor depends on the selection of the $B - H$ curve other than the core operating points [6]. In the end, the corresponding permeability of the core is decided.

The key element is a cylinder iron core which is wound by strips of grain oriented silicon steel and two kinds of windings are arranged orthogonally around the cylinder core. The inside winding is the bias coil connected to DC supply, the outside winding is the AC main coil connected to AC supply. The structural scheme is shown in Fig. 3.

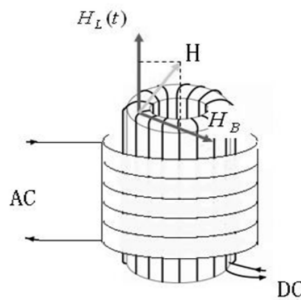


Fig. 3. Structure of the orthogonal core

Based on the above structure of the orthogonal core, AC main winding yields an AC flux in direction of the axis of the cylinder iron core when AC current is applied. The DC control winding is wound through the hollow cylinder and yields a DC flux along the azimuthal direction when DC current plus on. Subsequently, the AC flux and the DC flux are orthogonal in the cylinder core and a semi-rotating magnetic flux is formed. Fig. 4 shows a circumferential flux produced by DC current and axial flux generated by AC current.

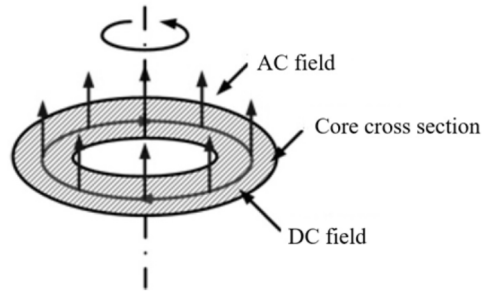


Fig. 4. Fluxes in the orthogonal core

The three-phase controllable reactor consists of two types of elements: up and down yokes which are wound by strips of grain oriented silicon steel and some control discs which are stocked as three-phase limbs (the number depends on the designed capacity). These control discs are wound also by silicon steel in the way of involute as shown in Fig. 5, which are the key elements for the three-phase reactor, playing the main role to determine the orthogonal flux and making the reactor controllable.

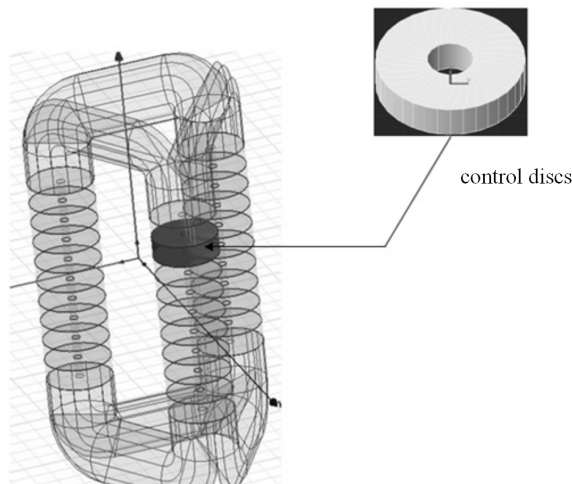


Fig. 5. Structure of three-phase controllable reactor

Each phase limb is the main core of the reactor as well as the return path of other

two phases' flux. For each phase core, AC current yields an AC flux in direction of the axis of the limb. In the meantime, DC current yields a DC flux along the annular direction. Subsequently, the AC flux and the DC flux are orthogonal in the control disc, and a semi-rotating magnetic flux is formed.

3. Result analysis and discussion

Generally, magnetic parameters of grain-oriented silicon steel is presented by magnetic permeability matrix without diagonal items of μ_{xx} and μ_{yy} [7]. However, when the grain-oriented core is subject to orthogonal field, the tensor permeability should be considered instead of above mentioned matrix. In the case a semi-rotating field is formed and the magnetic characteristics are different from that parallel field conditions, the following equation is used to describe the relationship between \mathbf{B} and \mathbf{H}

$$\begin{pmatrix} B_x \\ B_y \end{pmatrix} = \begin{bmatrix} \mu_{xx} & \mu_{xy} \\ \mu_{yx} & \mu_{yy} \end{bmatrix} \begin{pmatrix} H_x \\ H_y \end{pmatrix}. \quad (1)$$

When the inclination between \mathbf{H} and grain-oriented steel is different, the ratio of components of flux density B_x/B_y is different, and the permeability tensor is the function of the ratio [8]. The permeability matrix must include inclination items. These added items can be measured with two-dimensional excitation, the magnetic permeability is related to the inclination angle. As shown in Fig. 6.

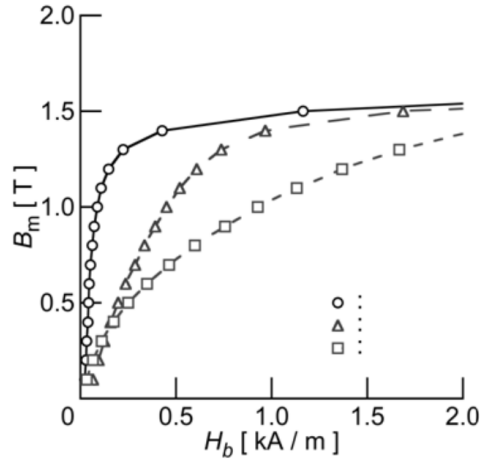


Fig. 6. Permeability relative with inclination angle

Furthermore, the tensor permeability is expressed as following:

$$\begin{pmatrix} \mu_{xx} \\ \mu_{xy} \\ \mu_{yx} \\ \mu_{yy} \end{pmatrix} = \begin{pmatrix} k_{11} & k_{12} & k_{13} & k_{14} \\ k_{21} & k_{22} & k_{23} & k_{24} \\ k_{31} & k_{32} & k_{33} & k_{34} \\ k_{41} & k_{42} & k_{43} & k_{44} \end{pmatrix} \begin{pmatrix} 1 \\ H_x^2 \\ H_x H_y \\ H_y^2 \end{pmatrix}, \quad (2)$$

where k_{ij} is the element of the coefficient matrix [9].

Let us setting AC exciting while $I_D = 0$, AC current creates magnetic field H_1 which establishes a magnetic field density B'_1 . The $B - H$ loop depends on the magnetization characteristics of the magnetic material. If H_1 is constant with I_D producing H_D , the composed field intensity becomes $\mathbf{H} = H_a \mathbf{e}_x + H_D \mathbf{e}_y$ where \mathbf{e}_x and \mathbf{e}_y are, respectively, the unit vectors in the H_a and H_D directions. The composed magnetic flux density \mathbf{B} is along with the direction of \mathbf{H} , and its value can be calculated from the $B - H$ curve.

The composed field \mathbf{B} can be divided into orthogonal components, as shown in Fig. 7. It is obvious to see $B_1 < B'_1$. Hence, the bias H_D is caused the variation of B'_1 to B_1 [10].

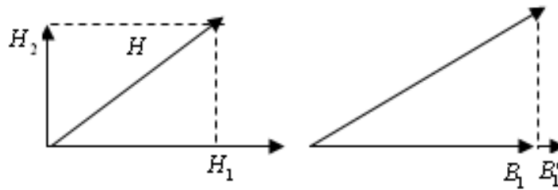


Fig. 7. DC bias field causes \mathbf{B} varying

It is clear that the two windings (AC winding and DC winding) are coupled through the tensor of permeability [11]. The DC current changes the $B - H$ curve in the plane into a new one and the magnetic behavior of the core depends on the new characteristics.

Considering the coupling among magnetic moments in the grain-oriented material, the energy E of the magnetic moment in an excitation field with the presence of an orthogonal bias field can be expressed as [12]

$$E = -\mu_0 (H_{\parallel} + H_{\perp} + \alpha M) , \tag{3}$$

where M is the magnetization, which is determined from both fields (AC flux and DC fluxes), and α is the magnetization coefficient. The resultant direction is not along the direction of the vector sum of the two \mathbf{H} fields.

The DC bias field generally reduces the magnetization in the AC flux direction. It is similar to an additional anisotropy along the orthogonal direction [13], and makes a perturbation of the original hysteresis along the excitation field.

When DC bias field is created, an additional anisotropy energy and elastic energy can be effectively calculated and included into the generalized anhysteretic function described previously [5]. The energy E of domains can be described as

$$E = -\mu_0 m (H_{\parallel} + H_{\perp} + \alpha M) + \tilde{E}_{\text{aniso}} + \tilde{E}_{\sigma} , \tag{4}$$

where \tilde{E}_{aniso} is the anisotropy energy and \tilde{E}_{σ} is the elastic energy.

From minimum energy theory, the magnetic material will get elastic distortion when the magnetization changes, so modeling of domain rotating can be established to analyze the system energy changing. All this phenomena are connected with

magneto mechanical field, which can be described as

$$E_{\text{total}} = E_H + \widetilde{E}_{\text{aniso}} + \widetilde{E}_{\sigma}, \quad (5)$$

where

$$\widetilde{E}_{\text{aniso}} = E_0 + K_1(\cos^2 \theta_1 \cos^2 \theta_2 + \cos^2 \theta_2 \cos^2 \theta_3 + \cos^2 \theta_3 \cos^2 \theta_1), \quad (6)$$

$$E_H = -\mu_0 M_s H (\cos \theta_1 \cos \phi_1 + \cos \theta_2 \cos \phi_2 + \cos \theta_3 \cos \phi_3), \quad (7)$$

$$\begin{aligned} \widetilde{E}_{\sigma} = & -\frac{3}{2} \lambda_{100} \sigma (\cos^2 \theta_1 \cos^2 \beta_1 + \cos^2 \theta_2 \cos^2 \beta_2 + \cos^2 \theta_3 \cos^2 \beta_3) - \\ & - \lambda_{111} \sigma (\cos \theta_1 \cos \theta_2 \cos \beta_1 \cos \beta_2 + \cos \theta_2 \cos \theta_3 \cos \beta_2 \cos \beta_3 + \\ & + \cos \theta_3 \cos \theta_1 \cos \beta_3 \cos \beta_1) \end{aligned} \quad (8)$$

and

$$\overline{\mu_{ij}} = \frac{1}{8\pi^2} \int_0^\pi \int_0^{2\pi} \int_0^{2\pi} \mu_{ij}(\theta, \varphi, \psi) \sin \theta \, d\psi \, d\varphi \, d\theta. \quad (9)$$

Here, E_H is the exciting field energy, $\theta_1, \phi_1, \beta_1$ are the angles between M, H , effective strain force and grain axial direction, respectively.

The magnetization equation now can be applied to calculate the above problem. After incorporation of the anisotropic and anhysteretic magnetization M_{aniso} , the magnetization curves can be calculated as the following functions:

$$\begin{aligned} \frac{dM}{dH} &= (1-c) \frac{M_{\text{an}} - M_{\text{irr}}}{k\delta - \alpha(M_{\text{an}} - M_{\text{irr}})} + c \frac{dM_{\text{an}}}{dH} \\ B_z &= \frac{\mu_0 M_{\text{sat}} H_z}{\sqrt{(H_z)^2 + (H_\varphi)^2}} + \mu_0 H_z. \end{aligned} \quad (10)$$

The relationship between M and H is given by “shearing” $M-H$ curves under different DC current biases through computer simulation.

Once the magnetization is obtained, the effective core permeability μ_{eff} may be found. Subsequently, the core inductance L can be obtained from the following approximate expression:

$$L \approx \frac{\mu_{\text{eff}} N_a^2 \pi (D^2 - d^2)}{4l}, \quad (11)$$

where N_a are the turns of the main coil, l is the core length, D and d are the out diameter and the inner diameter of the cylinder iron core, respectively.

A prototype of the proposed three-phase controllable reactor is fabricated, as shown in Fig. 8.

The overall size of the reactor is $600 \times 450 \times 500$ mm. The reactor body includes up yoke, down yoke and center limbs between the yokes. Each limb consists of 5

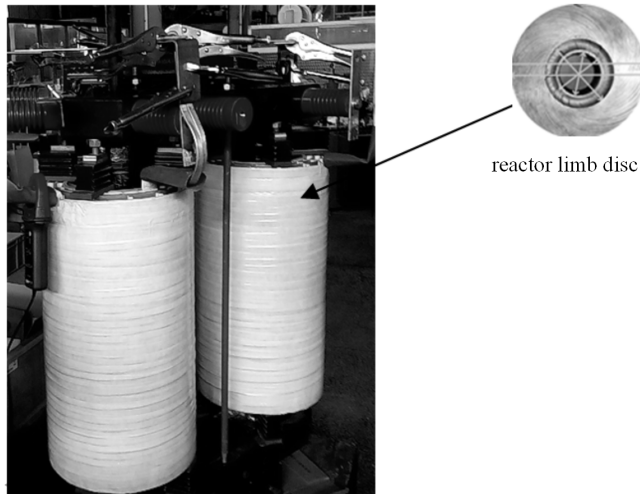


Fig. 8. Three-phase controllable reactor

control discs with outer diameter 160 mm and inner diameter 50 mm. The limb cylinder is with the parameters: $l = 250$ mm, $N_a = 250$ mm and $N_d = 100$ mm.

The prototype was investigated experimentally. The DC bias currents are adjusted to generate 0, 100, 200, 400 A/m orthogonal bias fields, separately. The effective inductance values of the prototype are shown in Fig. 9. It is obvious that the change of DC bias indeed leads to a change of the inductance value.

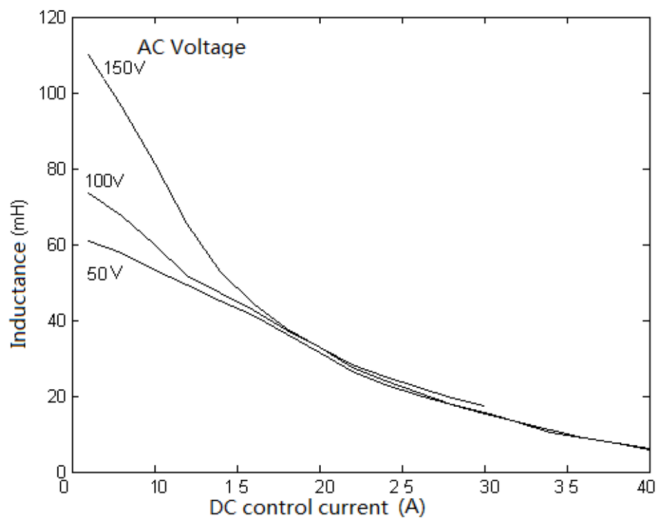


Fig. 9. Control characteristic of the reactor

In order to investigate the relationship between the orthogonal bias current and

the harmonic content, a further experiment was performed. When maintaining the main AC voltage 70 V and varying the orthogonal DC bias current from 0 A to 10 A, the work currents corresponding to different DC bias are gained. The corresponding harmonic analysis shows that with the increasing of the orthogonal bias current, the harmonic contents of the main current are relatively stable. This can be explained very well by the analysis above. The result indicates that variation of the orthogonal bias field does not only change the inductance, but may also lead to a good linearity of the inductance. It is a direction to develop a high quality controllable reactor [14].

4. Conclusion

Based on the quadrature magnetization, the three-phase controllable reactor can adjust the three-phase inductance under the influence of the DC bias current. The advantages of the new controllable reactor include:

- 1) Realization of the electrical insulation between AC voltage and DC control circuit to ensure the safety of the reactor, when using EVH or interference.
- 2) Three phase inductance can be adjusted at the same time, which secures balance of interests of the power grid and three-phase load change;
- 3) Low harmonics can adjust the three-phase inductance, and the current drives the corresponding iron core bias, which is much lower than the saturation point of the magnetic group". The advantage of low harmonic content is the reaction of high quality.
- 4) The magnetization mechanism can be described as changing the anisotropic magnetic field from the bias magnetic field, thereby providing additional energy for the anisotropy of the nucleus, thereby changing the effective permeability.
- 5) The new three-phase controllable reactor can be used for filtering or reactive power compensation.

References

- [1] S. SADTLER, B. LAUBE, A. LASUB, A. NICKE, H. BETZ, G. SCHMALZING: *A basic cluster determines topology of the cytoplasmic M3-M4 loop of the glycine receptor alpha1 subunit*. *Journal of Biological Chemistry* 278 (2003), No. 19, 16782–16790.
- [2] S. F. SHEN, Y. J. TANG, L. REN, Z. H. WANG: *Electromagnetic calculation of a 35 kV/3.5 MVA single-phase HTS controllable reactor with field-circuit coupled-FEM*. *IEEE Transactions on Applied Superconductivity* 26 (2016), No. 7, Article Sequence Number 5603305.
- [3] G. SUTTER, L. FAURE, A. MOLINARI, N. RANG, V. PINA: *An experimental technique for the measurement of temperature fields for the orthogonal cutting in high speed machining*. *International Journal of Machine Tools and Manufacture* 43 (2003), No. 7, 671–678.
- [4] X. CHEN, B. CHEN, C. TIAN, J. YUAN, Y. LIU: *Modeling and harmonic optimization of a two-stage saturable magnetically controlled reactor for an arc suppression coil*. *IEEE Transactions on Industrial Electronics* 59 (2012), No. 7, 2824–2831.
- [5] Y. WANG, S. ZHANG, G. CHEN: *A novel continuously adjustable magnetic-valve controllable reactor and its modeling*. *IEEE International Power Electronics and Motion*

- Control Conference, 2–5 June 2012, Harbin, China, IEEE Conference Publications 1 (2012), 77–80.
- [6] J. F. HOBURG, J. R. MELCHER: *Internal electrohydrodynamic instability and mixing of fluids with orthogonal field and conductivity gradients*. Journal of Fluid Mechanics 73 (1976), No. 2, 333–351.
 - [7] Q. YU, X. WANG, Y. CHENG: *Electromagnetic modeling and analysis of can effect of a canned induction electrical machine*. IEEE Transactions on Energy Conversion 31 (2016), No. 4, 1471–1478.
 - [8] M. S. MISRIKHANOV, A. O. MIRZABDULLAEV: *Analysis of the reasons for accidents and of protective measures against induced voltage on aerial electrical transmission lines*. Power Technology and Engineering 43 (2009), No. 1, 54–59.
 - [9] R. P. VERMA, W. Z. FAM: *Theory and performance of parametric transformers*. IEEE Transactions on Power Apparatus and Systems PAS-91 (1972), No. 6, 2494–2504.
 - [10] J. H. CITRINITI, W. K. GEORGE: *Reconstruction of global velocity field on the axisymmetric mixing layer utilizing proper orthogonal decomposition*. Journal of Fluid Mechanics 418, (2000), 137–166.
 - [11] T. XU, J. T. GOLDBACH, T. P. RUSSELL: *Sequential, orthogonal fields: A path to long-range, 3-D order in block copolymer thin films*. Macromolecules 36 (2003), No. 19, 7296–7300.
 - [12] C. DINC, I. LAZOGLU, A. SERPENGUZEL: *Analysis of thermal fields in orthogonal machining with infrared imaging*. Journal of Materials Processing Technology 198 (2008), Nos. 1–3, 147–154.
 - [13] T. SONDERGAARD, P. F. J. LERMUSIAUX: *Data assimilation with gaussian mixture models using the dynamically orthogonal field equations. Part II: Applications*. American Meteorological Society, Monthly Weather Review 141, (2013), No. 6, 1761–1785.
 - [14] Z. H. WANG, Y. J. TANG, L. REN, S. YAN, Z. G. YANG, Y. XU, C. ZHANG: *Development of a new type of HTS controllable reactor with orthogonally configured core*. IEEE Transactions on Applied Superconductivity 27 (2017), No. 4, Article Sequence Number 5000205.

Received September 19, 2017

